La mer 26: 99-114, 1988
Société franco-japonaise d'océanographie, Tokyo

Coastal and bottom topographic effects on the path dynamics of the western boundary current with special reference to the Kuroshio south of Japan*

Yoshihiko SEKINE**

Abstract: The Kuroshio region south of Japan is characterized by a small coastline inclination from west-east direction and narrow continental slope in comparison with other western boundary currents. The Kuroshio shows bimodal path characteristics between large meander and no meander path, but the large meander path is not observed in other western boundary currents. A barotropic numerical model is used to study the coastal and bottom topographic effects on the path dynamics of the Kuroshio in the present study. It is shown by a flat model that a western boundary current along a zonal northern coast has a tendency to generate a large meander path. Conversely a western boundary current along a coast with larger coastline inclination from W-E direction apts to flow along the northern boundary, in which if both a small horizontal eddy viscosity and a large in- and outflow transport are imposed, an instability of the coastal flow is carried out and a separation of the current path is formed. It is also demonstrated that if the topographic effect of the continental slope is included in a model, it suppresses the formation of the meander path by the topographic guiding effect along the geostrophic contour. These results indicate that the formation of the large meander path is strongly connected with the instability of the frictional boundary layer current along the coast. If the instability occurs and the relative vorticity advected offshore region by the mean flow is balanced with the Rossby wave motion, a meander path is formed. These results indicate that zonal coastal boundary and steep narrow continental slope found in south to Japan have a larger possibility to form a large meander path than those of other western boundary currents.

1. Introduction

The Kuroshio is a western boundary current in the North Pacific. It has been widely accepted that the Kuroshio takes one of the two relatively stable paths south of Japan, which is known as bimodal path characteristics. One stable path is rather straight and it is referred to as no large meander path. Another path exhibits a large meander south of Japan and it is referred to as large meander path (e.g. STOMMEL and YOSHIDA, 1972; NISHIDA, 1982; ISHII *et al.*, 1983). Recently, KAWABE (1985) showed by the analysis of the sea level data at the Izu Islands that the Kuroshio takes a large meander path about 40% of the total time period and the no meander path is furthermore divided into two types referred to as nearshore and offshore non-large-meander paths. It should be noted here that the large meander path is peculiar to the Kuroshio south of Japan and similar phenomenon is not observed in the other western boundary currents.

Fig. 1 (a) shows the topographic features south of Japan. If we compare this topography with those of other two representative western boundary regions shown in (b), it is noted that the Kuroshio region south of Japan has some characteristic features of the coastal and bottom topographies. (1) The existence of the Izu Ridge is peculiar and its topography rises up from a flat basin to block the Kuroshio flowing over it. (2) A coastline inclination from west-east direction is relatively small in south of Japan, in particular from Shikoku to the Boso

* Received April 21, 1988
** Institute of Geosciences, National Defense Academy, Yokosuka, 239 Japan
Present address: Institute of Oceanography, Faculty of Bioresources, Mie University, Kamihama-cho 1515, Tsu, Mie, 514 Japan

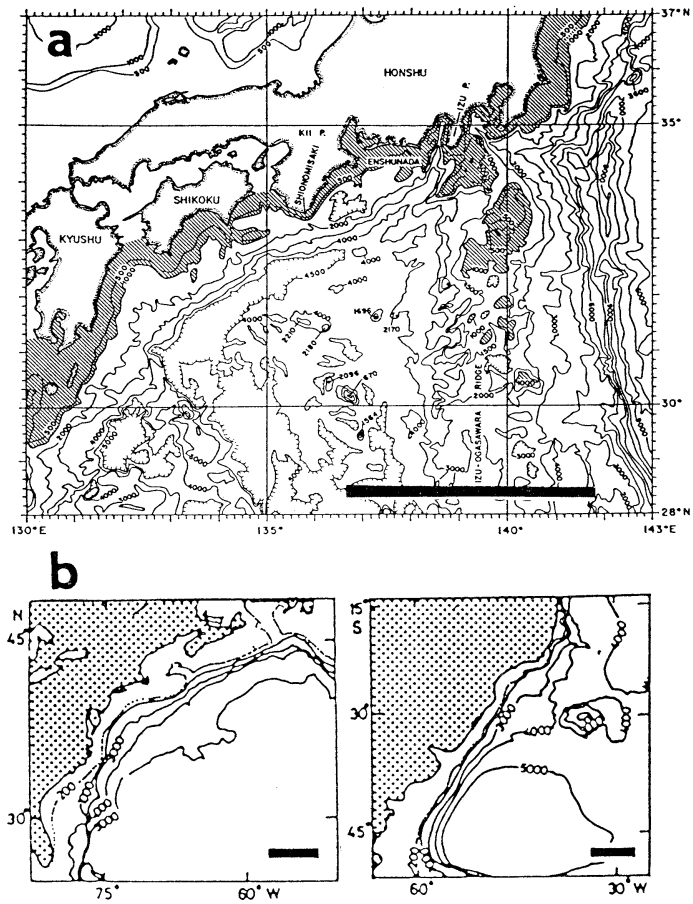

Fig. 1. Bathymetric chart of the three western boundary regions (a) south of Japan (after TAFT, 1972), (b) east of the North America (left) and east of the South America (right). The solid bands in right bottom show the distance of 500 km in each panel.

Peninsula. In contrast to this, the coastline inclinations of other western boundary currents are relatively large (see Fig. 1b). (3) The width of the continental slope is relatively small in south of Japan. Namely, the averaged width of the continental slope south of Japan is about one third of that of the Florida Current region. Considering that the appearance of the large meander path is peculiar to the Kuroshio, there is a possibility that the large meander path is caused by the characteristic coastal and bottom topographies south of Japan mentioned above.

So far, many authors have investigated the path dynamics of the Kuroshio south of Japan. As for the topographic effect of the Izu Ridge denoted in the item (1), because the relatively deeper region over the Izu Ridge exists between the two islands, the Hachijo-jima and the Miyake-jima, the Kuroshio has a tendency to pass this region, which has been referred to as the gate effect of the Izu Ridge (cf. WHITE and MCCREARY, 1976). The gate effect was studied by some authors (e.g. MASUDA, 1982; CHAO and MCCREARY, 1982; CHAO, 1984; YASUDA *et al.*, 1985). However, recent sea level analysis by OTSUKA (1985) suggested that the axis of the Kuroshio is not confined to the gate region over the Izu Ridge.

As for the topographic effect of the continental slope denoted in the item (3), many authors have studied by use of various models (e.g. ROBINSON and TAFT, 1972; ENDOH, 1973,

1979; SEKINE, 1979, 1980; SEKINE and TOBA, 1980; MIURA and SUGINOHARA, 1982) and commonly pointed out that if the lower layer motion touching the bottom slope exists, the topographic guiding effect on the current to flow along an isopleth of the depth is prominent. Recent direct current measurements have clarified the prominent velocity in the lower layer (e.g. FUKASAWA and TERAMOTO, 1986) and it suggests that the topographic effect may not be neglected in the path dynamics of the Kuroshio. Recent numerical model with the realistic continental slope and the Izu Ridge (SEKINE, 1989a, b) demonstrates an impotant role of the topographic effect of the Izu Ridge and the continental slope south of Japan. In particular, SEKINE (1989b) pointed out that the formation of the large meander path is confined to a narrow parameter range over the continental slope, but a large meander path dominates if a flat bottom basin is assumed.

Recently, CHAO (1984), SEKINE (1984) and YOON and YASUDA (1987) made numerical experiments with an inclined coastal boundary from W-E direction denoted in the item (2). It has been commonly demonstrated that the occurrence of the large meander path is carried out in larger volume transport in comparison with the case of the zonal coastal boundary. However, the parameter dependence of the model ocean has not fully been performed in the models of CHAO (1984). More detailed study on the coastline inclination was made by YOON and YASUDA (1987). But their model has some shortcomings; a topographic effect of the continental slope and the model dependence on the intensity of eddy viscosity has not been considered. Furthermore, because their model covers only the Shikoku Basin and the eastward outflow is made at the gate region of the Izu Ridge, the current path not through the gate region represented by the offshore non-large-meander path (cf. KAWABE, 1985) is omitted in the discussion.

In the present study, the topographic effect of the coastline inclination and continental slope is examined by use of a simplified numerical model. Emphasis is placed on the association with the topographic effect of the continental slope, the dependence of the intensity of eddy viscosity and the volume transport of the in- and outflow. It will be shown that the condition on the appearance of the large meander path is very complicated and the clear observational verification of model parameters is needed to draw a firm conclusion on the path dynamics of the Kuroshio south of Japan.

2. The model

In order to see the specified roles of the coastline inclination, the continental slope and other physical parameters, eleven runs with different model and/or the model parameters are performed (see Table 1). Barotropic model is assumed for all the cases. Schematic view of the model ocean is shown in Fig. 2.

In the first phase, a flat bottom with a depth

Table 1. The parameters, coastal and bottom topographies, and boundary in- and outflow transport for the experiments discussed in this study.

Run no.	Coastal topography (Tilt of the coast from the E-W direction in degree)	Continental slope, Δh (m)	Total transport of inflow (Sv)	Horizontal dissipation, A_h ($cm^2 s^{-1}$)
1	0°	0	40	5×10^6
2	10°	0	40	5×10^6
3	20°	0	40	5×10^6
4	30°	0	40	5×10^6
5	0°	100	40	5×10^6
6	0°	200	40	5×10^6
7	0°	500	40	5×10^6
8	30°	0	100	5×10^6
9	30°	0	150	5×10^6
10	30°	0	100	10^6
11	30°	0	100	5×10^5

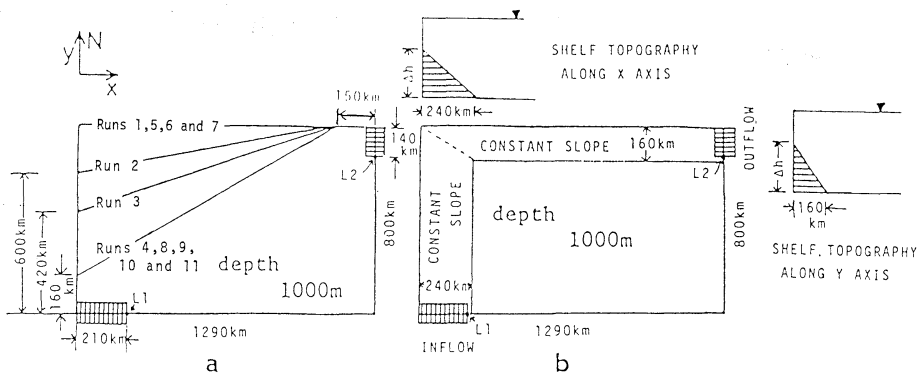

Fig. 2. (a) Schematic view of the flat bottom model with four different northern coastal boundaries. (b) Schematic view of the model with the constant continental slope. Two sections of the bottom topography are also shown in top and right. Δh is changed in three runs (see Table 1).

of 1,000 m is assumed and only the northern coastal inclination is changed among Runs 1-4 (see Table 1). The straight line drawn from the Tokara Strait to the Boso Peninsula has an angle of about 30 degrees from W-E direction (see Fig. 1) and this angle is similar to those of the model employed in Runs 4 and 8-11. If the coastline between the west of Shikoku and the Boso Peninsula is considered, the coastline inclination decreases to about 20 degrees, which is similar to that of Run 2. In the second phase, the specified topographic effect of the continental slope is examined. In these models, the rectangular basin is assumed and only the gradient of constant slope is changed among Runs 5-7 (see Fig. 2(b)). Here, since the bottom effect of the continental slope is studied, the effect of the Izu Ridge is excluded. The effect of the Izu Ridge will be studied in the succeeding paper (SEKINE, MS) with reference to the multiple steady state of the current path. On the basis of the results of previous two phases, the condition on the appearance of the large meander path in a large coastline inclination is checked in the third phase; a specified large nonlinear effect by large in- and outflow is given in Runs 8 and 9 and a smaller eddy viscosity is given in Runs 10 and 11.

In all runs, the system is driven by an inflow and outflow through the boundary. The inflow is given at the western part of the southern boundary corresponding to the southeast off Kyushu. In order to include the offshore non-large-meander path, the outflow is carried out at the eastern boundary corresponding to southeastern region off the Boso Peninsula. Basic equations are vertically integrated vorticity equations under the hydrostatic balance and the beta plane approximation:

Table 2. List of symbols.

x	eastward component of Cartesian coordinate
y	northward component of Cartesian coordinate
u	x-directed (eastward) component of velocity
v	y-directed (northward) component of velocity
z	relative vorticity
ϕ	volume transport function (stream function)
h	depth of the ocean
f	Coriolis parameter ($f=f_0+\beta y$, $f_0=7\times10^{-5}\ s^{-1}$)
β	factor in Coriolis parameter ($=2\times10^{-13}\ s^{-1}\ cm^{-1}$)
A_h	coefficient of horizontal eddy viscosity
∇^2	horizontal Laplacian operator $\left(=\frac{\partial^2}{\partial x^2}+\frac{\partial^2}{\partial y^2}\right)$

$$\underbrace{\frac{\partial z}{\partial t}}_{T_c}=\underbrace{-\frac{\partial uz}{\partial x}}_{J_x}\underbrace{-\frac{\partial vz}{\partial y}}_{J_y}\underbrace{-\beta v}_{B}-\underbrace{f\left(\frac{\partial u}{\partial x}+\frac{\partial v}{\partial y}\right)}_{Div.}+\underbrace{A_h\nabla^2 z}_{Fr}, \qquad (1)$$

$$z=\frac{\partial v}{\partial x}-\frac{\partial u}{\partial y}=\frac{\partial}{\partial x}\left(\frac{1}{h}\frac{\partial \phi}{\partial x}\right)+\frac{\partial}{\partial y}\left(\frac{1}{h}\frac{\partial \phi}{\partial y}\right), \qquad (2)$$

where all the symbols are listed in Table 2. A slip boundary condition is imposed at the southern

and eastern boundaries and a viscous boundary condition is assumed at the western and northern boundaries. The equations (1) and (2) are solved numerically with the grid resolution of 30 km (east-west) and 20 km (south-north) for Runs 1–9 and the resolution of 15 km (east-west) and 10 km (south-north) for Runs 10 and 11 with the smaller horizontal eddy viscosity. A leap frog scheme is basically used in the finite form of the local time change and an Euler backward scheme (MATSUNO, 1966) at every 20 time step is employed to suppress the growth of computational modes. The space difference form of (1) is the same as in BRYAN (1963) and the Poisson equation (2) is solved by the successive over relaxation method.

Stationary in- and outflow are assumed at the boundary and a sinusoidal form of the horizontal velocity distribution is employed. Boundary conditions at the inflow southern boundary ($y=0$ km) are

$$\left.\begin{aligned}\phi&=\phi_0-\phi_0\cos\left(\frac{\pi}{L_1}x\right) \quad \text{for } 0\leq x\leq L_1,\\ \phi&=2\phi_0 \qquad\qquad \text{for } L_1<x\leq 1290\,\text{km},\end{aligned}\right\} \quad (3)$$

where ϕ_0 is a half of the total transport of the in- and outflow, and L_1 ($=210$ km) is the width of the inflow (see Fig. 2). The similar boundary condition is imposed at the eastern outflow boundary ($x=1{,}290$ km),

$$\left.\begin{aligned}\phi&=2\phi_0 \qquad\qquad \text{for } 0\leq y\leq 660\,\text{km},\\ \phi&=\phi_0+\phi_0\cos\left[\frac{\pi}{L_2}(y-660)\right]\\ &\qquad\qquad \text{for } 660\,\text{km}<y\leq 800\,\text{km},\end{aligned}\right\} \quad (4)$$

where L_2 ($=140$ km) is the width of the outflow. In all runs, the volume transport function at an initial stage is set to be parallel to the western and northern boundaries and it will be also shown together with the results of time integrated numerical solutions.

3. Results

3.1. *The effect of the coastline inclination from W-E direction on the western boundary current (Runs 1 to 4)*

The results of Runs 1 to 4 with different northern boundary are shown in Fig. 3. The time variation of Run 1 depicts that a small current separation from the northern boundary is formed gradually by the lapse of time and a cyclonic circulation appears in its coastal side. The large meander flow pattern of Run 1 with a cyclonic eddy shown by the negative transport function between two anticyclonic circulation is almost similar to the observed large meander of the Kuroshio south of Japan.

The results of Run 2 show that an initial straight path forms meander patterns more slowly, but some different meander patterns are perceived in comparison with those of Run 1. The separation of the current path from the northern boundary is carried out in the downstream region and the current path flows zonally for a long distance from the western boundary. So, the generated coupled anticyclonic and cyclonic circulations have longer zonal diameter. If the meander patterns in Runs 1 and 2 are assumed to be stationary Rossby waves, their wavelengths are evaluated, $2\pi\sqrt{U/\beta}$ for Run 1 and $2\pi\sqrt{U\cos(10°)/\beta}$ for Run 2. It is thus suggested that the stationary Rossby wave has shorter wavelength in Run 2 by a factor of $\sqrt{\cos(10°)}$. However, this contradicts with the present results showing that the wavelength of Run 2 is longer than that of Run 1. This contradiction is caused by the neglect of the effect of northern boundary, and if the boundary effect is considered, the Rossby wave can not behave as in an open area. It is pointed out that the stationary Rossby wave theory (e.g. WHITE and MCCREARY, 1976) is applicable only in the open ocean and to include the effect of coastal boundary is needed in the dynamics of the large meander path. The total flow pattern of Run 2 resembles the observed offshore non-large meander path classified by KAWABE (1985).

The results of Runs 3 and 4 show that the initial current path furthermore shifts westward and a narrow coastal current along the northern boundary is formed. Although some small eddies are formed in south of the main current path, they give no major influences on the time evolution of the current path. These results demonstrate that formation of the large meander path is strongly suppressed in Runs 3 and 4. It should be also noted that northward flows along a western boundary in Runs 1 and 2 are stable and they continue to flow along the boundary. In summary, a western boundary current along a larger coastline inclination from W-E direc-

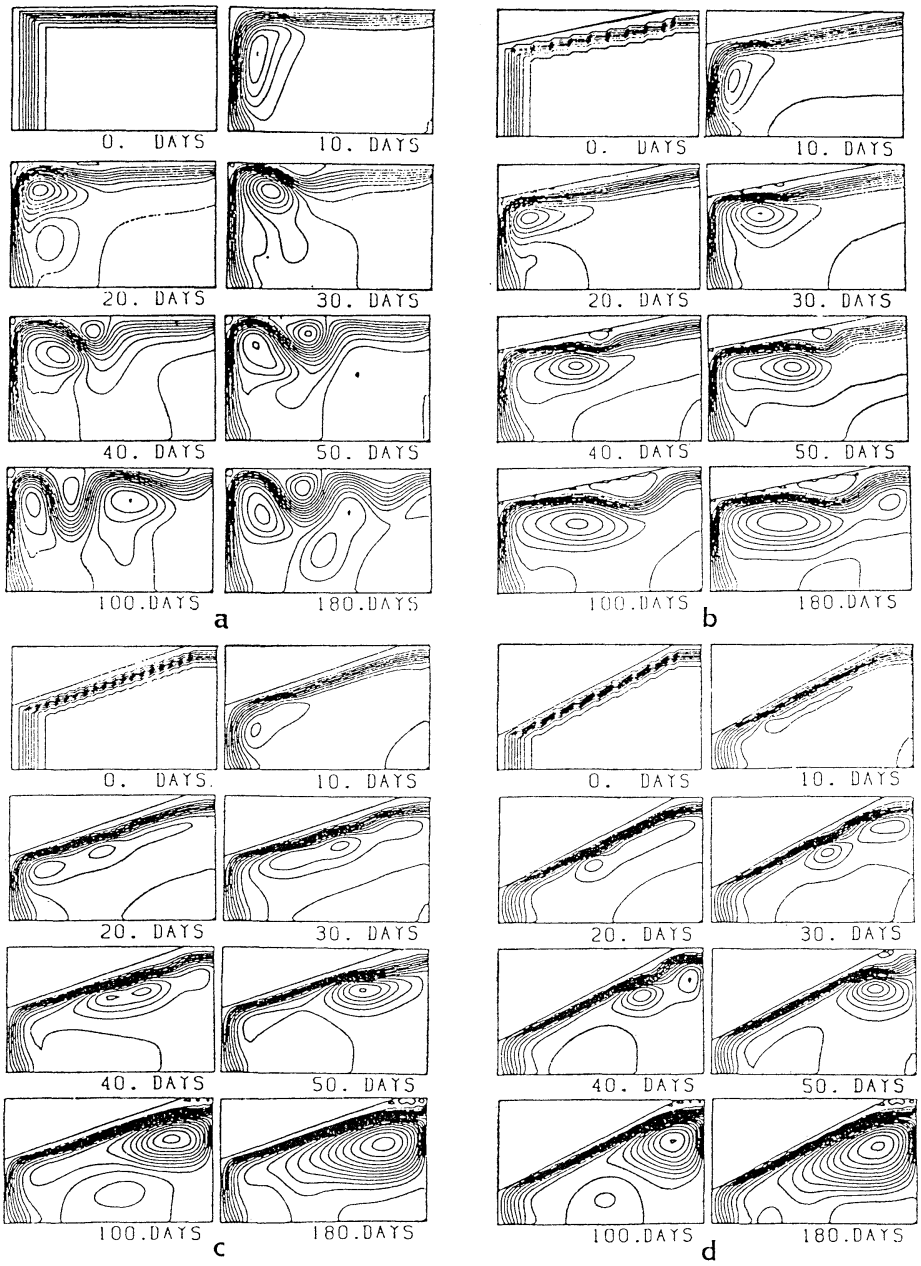

Fig. 3. Results of numerical experiments shown by the sequential pattern of total volume transport function. (a) Run 1, (b) Run 2, (c) Run 3 and (d) Run 4. Contour interval of the two neighbouring volume transport function is 5 Sv and the region with the negative transport function is stippled.

tion has a stronger tendency to flow along the coastal boundary in comparison with those along zonal coastal boundary.

To see the difference in the coastal boundary effect, Fig. 4 compares the time variation of the term balance in the vorticity equation (1) between Runs 1 and 4. One point, referred to as ***i*** point, is in the coastal side of the main current

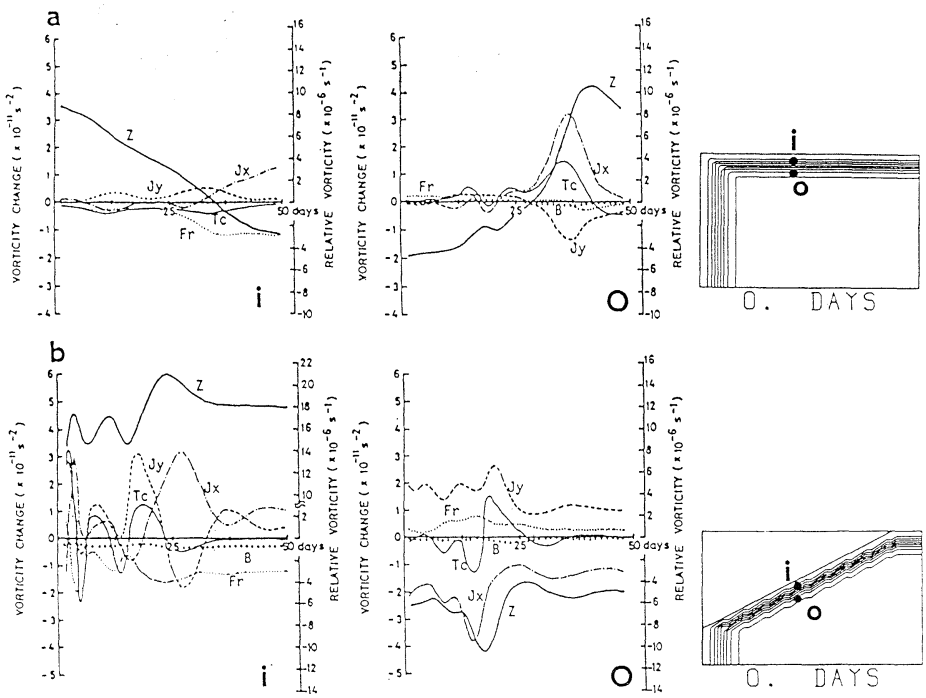

Fig. 4. Time change in the relative vorticity and five terms in the vorticity equation (1) at the two points. The distance of the two points from the northern boundary is 20 km for ***i*** point and 120 km for ***o*** point. The zonal position of the two points, which are shown in the right of figures, is middle of the oblique coastal boundary (x=540 km from the western boundary). (a) Run 1, and (b) Run 4. Z, Jx, Jy, Fr, B and Tc show the relative vorticity, eastward and northward vorticity advection, horizontal eddy viscosity, planetary beta and total vorticity change (local change) terms in (1), respectively.

axis, where positive vorticity is given in the initial condition, while the other ***o*** point is in the offshore side of the main current axis with the negative vorticity in the initial stage (for the position of these two points, see right map in Fig. 4). At the ***i*** point of Run 1, three terms show poor compensation and no stable vorticity balance is achieved; the total vorticity change $\partial z/\partial t$ is always negative and the relative vorticity changes from positive to negative at about 30th day. In contrast to this, the vorticity change at ***i*** point of Run 4 shows oscillating feature between the positive and negative values and it becomes stationary (nearly zero) after about 30th day: the stationary vorticity balance is made among two positive nonlinear terms and the negative friction and planetary beta terms.

At the ***o*** point of Run 1, the prominent positive nonlinear term $-\partial uz/\partial x$ contributes to make the relative vorticity positive. However, at the ***o*** point of Run 4, the time variation in the relative vorticity is rather small due to the balance of the four terms in (1). An apparent local time change of Run 4 is detected in 15–20 days, when the passage of an anticyclonic eddy in the offshore side of the main current axis is perceived (see Fig. 3). After the 30th day, stable vorticity balance is established among the positive friction and one of the nonlinear term $-\partial vz/\partial y$ and the two other negative terms. The planetary beta term is secondary. The stationary flow pattern of Run 4 is due to this stable vorticity balance.

Another possible cause of the difference in the results between Runs 1 and 4 is originated in the deformation of the current path at the western north corner of the model ocean. In Run 1 larger positive vorticity (cyclonic circulation) is given in the mean flow at the western north corner, while the corresponding vorticity

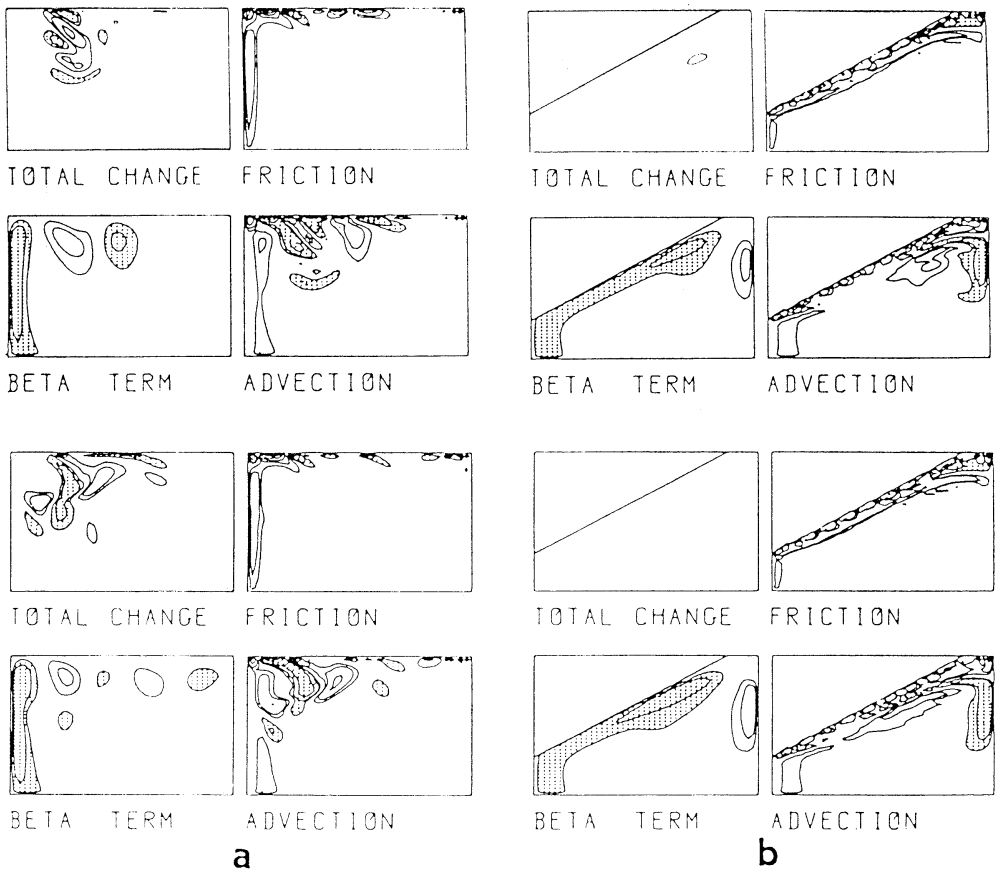

Fig. 5. Spatial vorticity balance at the 50th day (upper four panels) and at the 100th day (lower four panels). (a) Run 1 and (b) Run 4. Contour interval is $5\times10^{-12}s^{-2}$ and the regions with negative vorticity change are stippled.

change in Run 4 is relatively small due to the smaller deflection of the mean flow.

Fig. 5 compares spatial distribution of the term balance in (1) between Runs 1 and 4 at the 50th and 100th day. Fig. 5 shows that the friction term is important near the coastal boundary and the planetary beta term is dominant along the western boundary, while the nonlinear term is noticeable along the main current axis. In both runs, the northward flow along western boundary has a vorticity balance between the planetary beta term and the friction term in the coastal side of the main current axis, but it changes to balance between the beta term and advection term in its offshore side; the frictional boundary current (MUNK, 1950) is suggested for the former case and the inertial boundary current (e.g. MUNK *et al.*, 1950) for the latter case (for the relationship between the frictional and inertial western boundary currents, see VERONIS, 1966). It is suggested from Figs. 4 and 5 that the advection term is dominant in the offshore region in Run 1 and it yields remarkable total vorticity change ($\partial z/\partial t$) there. This means that the initial coastal flow in Run 1 is unstable. In contrast to this, the time change ($\partial z/\partial t$) is very small in Run 4 because of the vorticity balance among advection, friction and beta terms, and it means that the initial current path along the boundary is stable.

3.2. *The topographic effect of the continental slope (Runs 5-7)*

The results of Runs 5-7 with the continental slope are shown in Fig. 6. Because of the longer

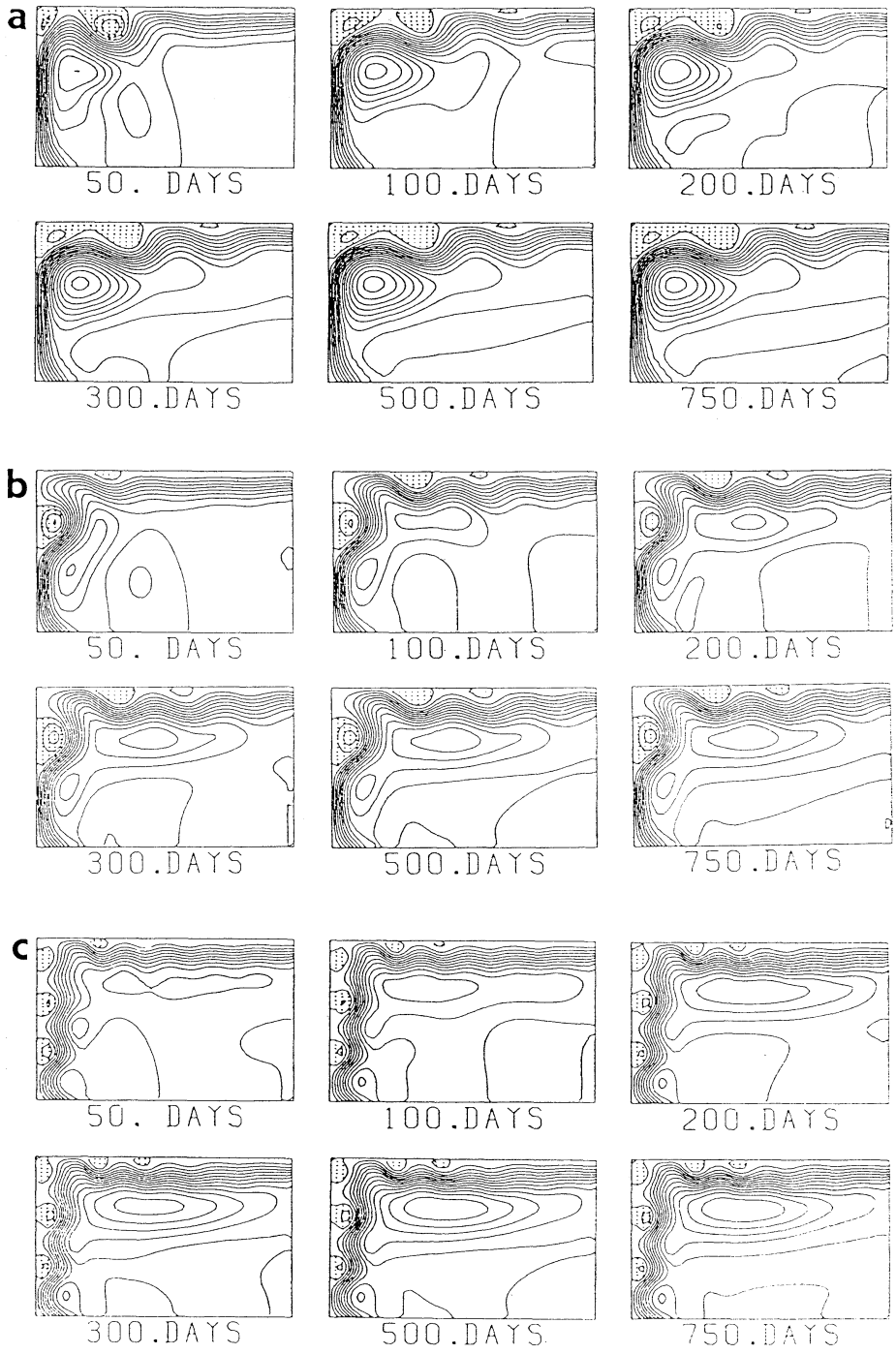

Fig. 6. The same as in Fig. 3, but for (a) Run 5, (b) Run 6 and (c) Run 7.

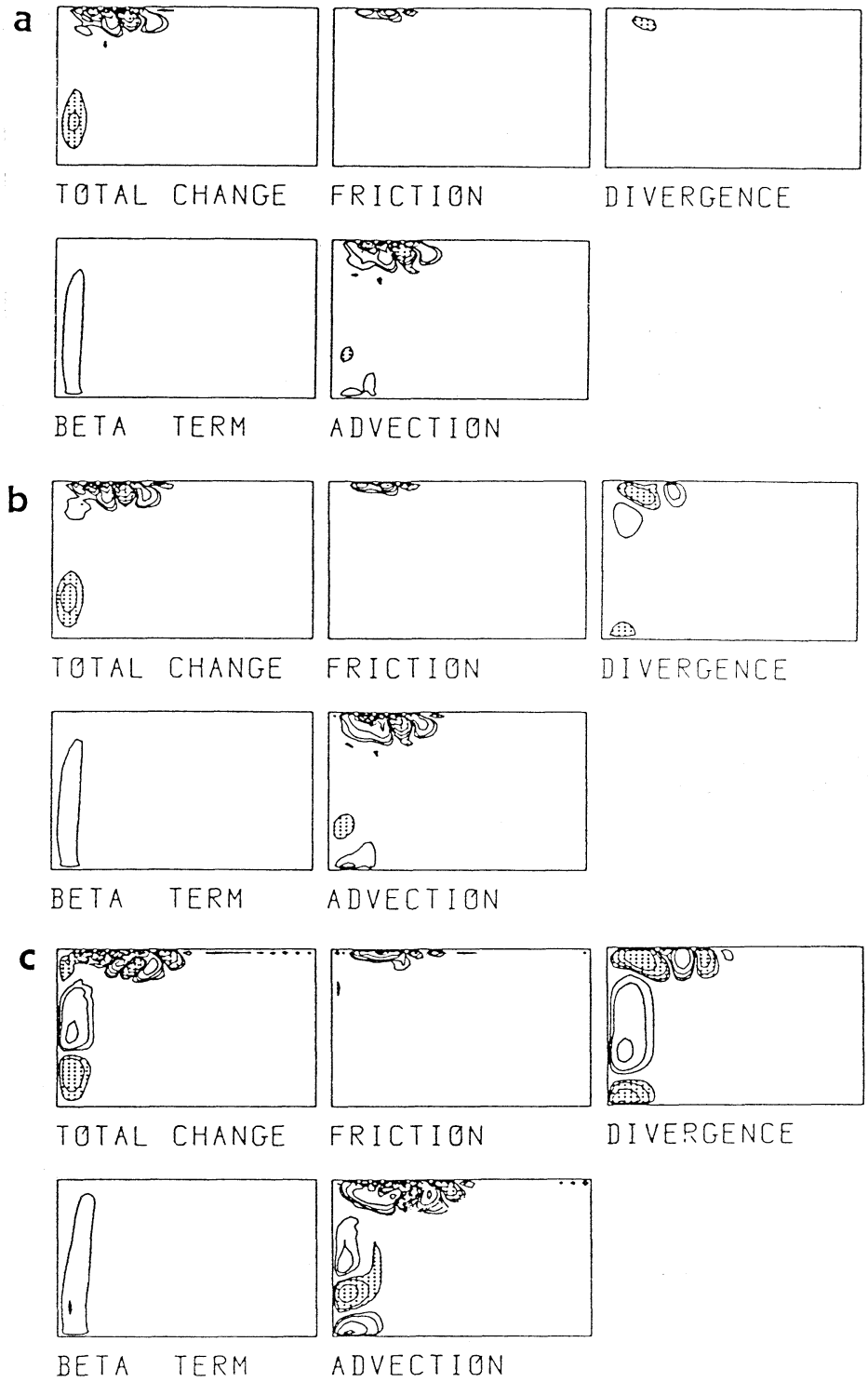

Fig. 7. Spatial vorticity balance at the 5th day. (a) Run 5, (b) Run 6 and (c) Run 7. Contour interval is the same as in Fig. 5.

time response of the topographic Rossby wave, the numerical integration is carried out upto 750th day. A meander of the current path is perceived in Run 5, but the amplitude of the meander is smaller than that of Run 1. Because the topographic effect of the continental slope is more prominent in Runs 6 and 7, the main current path has a tendency to flow over the continental slope. The amplitude of meander decreases from Run 5 to Run 7, and it is clear that the existence of a steeper continental slope suppresses the development of the meander path more remarkably. The different flow pattern of Runs 6 and 7 from that of Run 5 is a generation of eddies along the western boundary. These eddies act as a southward topographic Rossby wave in the northward mean flow.

The vorticity balance of these three runs at the 5th day is shown in Fig. 7. In Run 5, the time change $\partial z/\partial t$ is mainly due to advection term, while the topographic divergence term is relatively small. However, as the gradient of the continental slope is increased, the divergence term becomes important in the vorticity balance. In particular, the total time change in Run 7 is mainly due to the divergence term and it forces

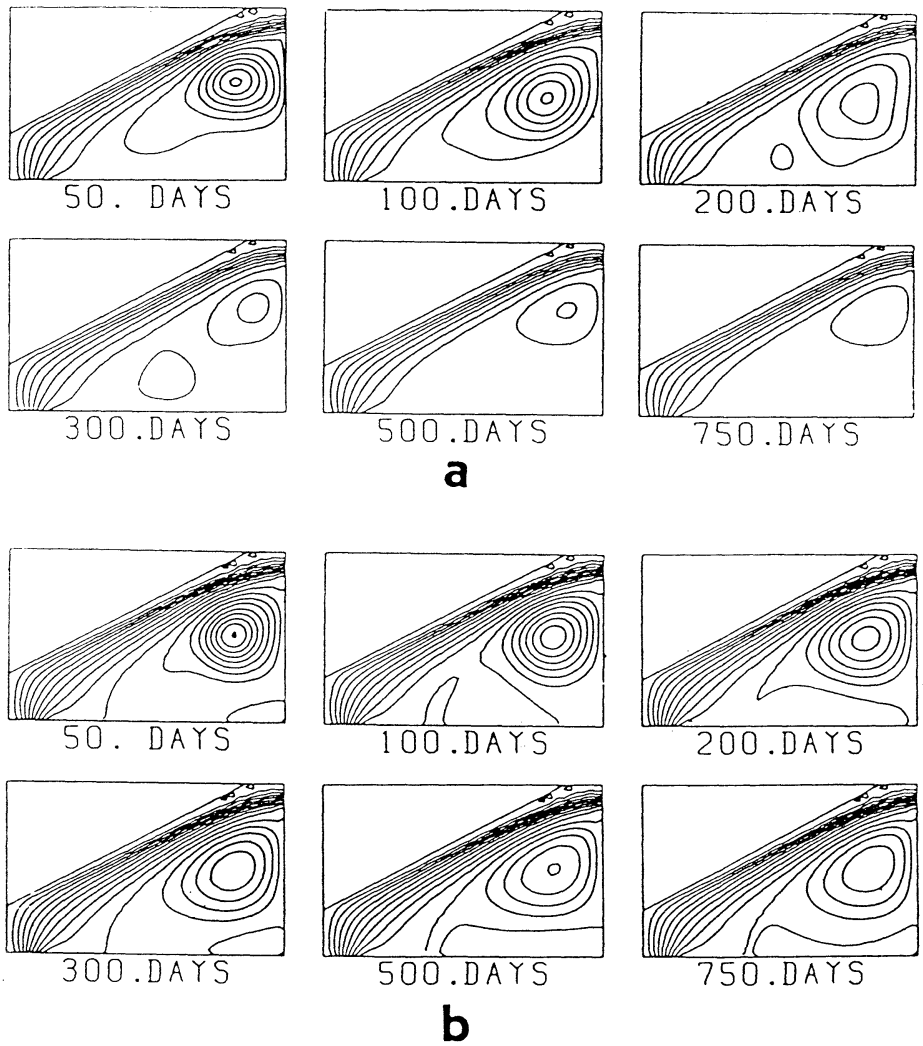

Fig. 8. Results of numerical experiment. (a) Run 8, and (b) Run 9. Contour interval of the volume transport function is 15 Sv.

the current path to flow along the geostrophic contour (f/h), which is well approximated by the isopleth of the depth (h). In comparison with the results of the flat bottom model shown in Fig. 3, these models show that even in a model with zonal northern boundary, the formation of the large meander path is suppressed, if the topographic effect is remarkable. It is thus suggested that the appearance of the large meander path in the Kuroshio flow is associated with the fact that topographic effect of the continental slope is confined to the narrow continental slope south of Japan (see Fig. 1).

3.3. *The effect of large in- and outflow volume transport (Runs 8 and 9)*

In order to see the condition on the appearance of the large meander path in the model with large coastline inclination, the large in- and outflow volume transports of 100 Sv and 150 Sv are given in Runs 8 and 9, respectively (Table 1). The results of these two runs are displayed in Fig. 8. It is shown that initial current paths of both runs along the northern boundary are maintained stationary and the total flow pattern shows no prominent difference from those of Run 4.

Vorticity balances of Run 9 along $x=540$ km at two times are shown in Fig. 9. Vorticity balance is made by the two dominant nonlinear terms $-\partial zu/\partial x$ and $-\partial zv/\partial y$. But the two terms compensate each other and the total nonlinear effect on the time change $\partial z/\partial t$ is small. Beta term and friction term are secondary. Therefore, total time change of the relative vorticity $\partial z/\partial t$ is very small and it results in no apparent change of the initial current path along the northern boundary. Provided that the observed maximum volume transport of the Kuroshio is less than 150 Sv, the increase in the volume transport yields no large meander path in the large coastline inclination of 30°.

3.4. *Effect of small horizontal dissipation (Runs 10 and 11)*

The condition on the appearance of large meander path in the large coastline inclination is furthermore checked by the model with a small coefficient of the horizontal eddy viscosity. The results of Runs 10 and 11 are displayed in Fig. 10. The width of the western boundary current in Run 10 is smaller than Run 8 with the same in- and outflow. This is due to the decrease in the horizontal eddy viscosity. In Run 10, although weak current separations are noticed, the total flow pattern indicates the predominance of the no meander path along the coast.

Results of Run 11 show that the flow patterns at 50th day are almost similar to those with the larger horizontal dissipation, but some

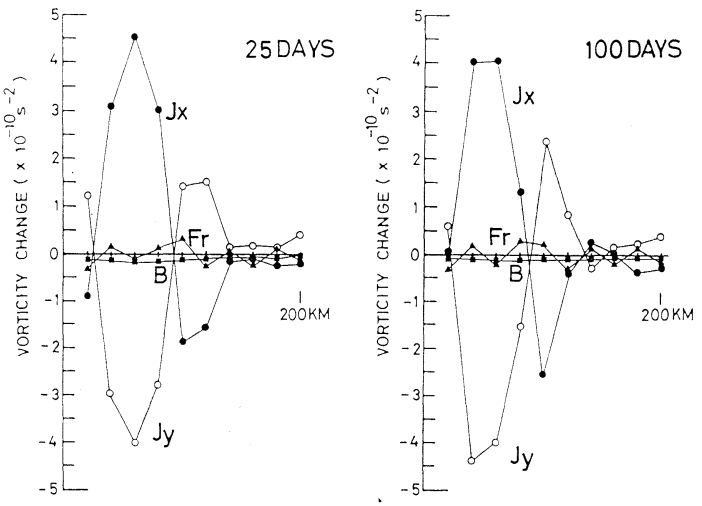

Fig. 9. Vorticity balance of Run 6 along the meridional line passing ***o*** and ***i*** points shown in Fig. 4 ($x=540$ km from the western boundary). Zonal axis shows the distance from the northern boundary.

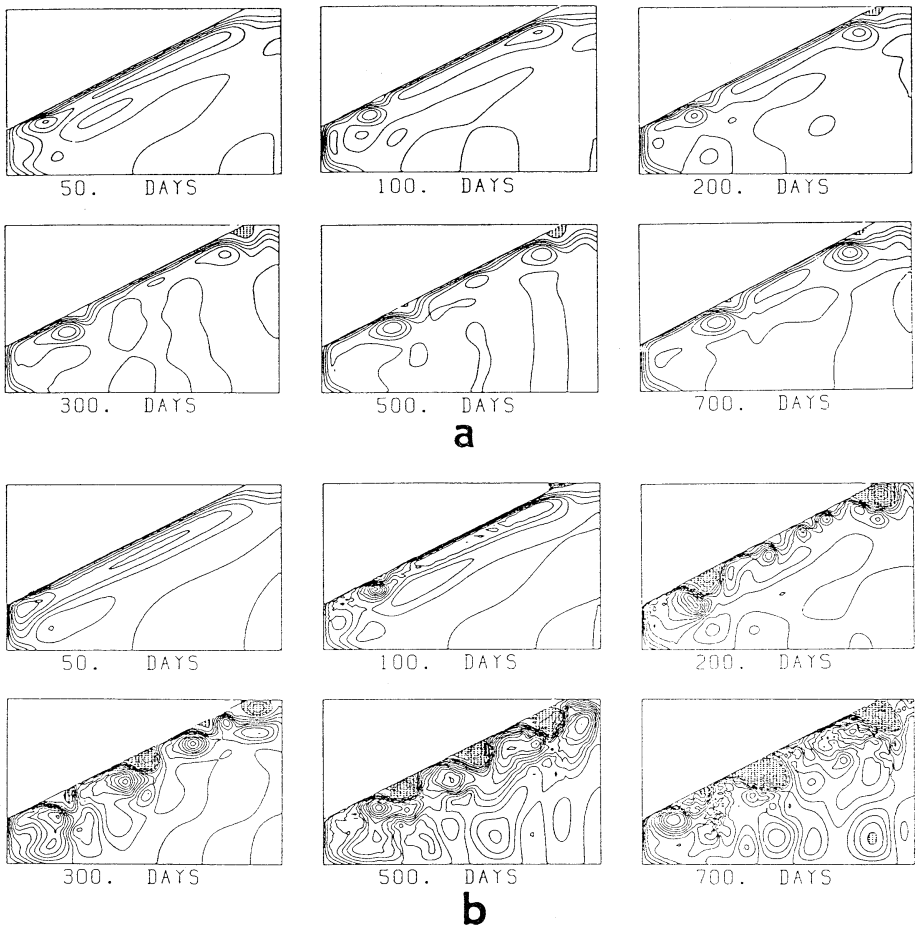

Fig. 10. The same as in Fig. 8, but for (a) Run 10 and (b) Run 11. Contour interval of the volume transport function is 25 Sv.

unstable eddies appear at about 200th day. The clear difference of the flow pattern of Run 11 from that of Run 10 is the development of cylonic and anticyclonic circulations along the coast. By the development of these eddies, the meander of the current path is formed by the lapse of time. The meander path is not stationary and its wavelength becomes larger gradually. In order to see the difference in the results of Run 11 from those of Runs 8 and 9, the vorticity balance of Run 11 is shown in Fig. 11. The two dominant nonlinear terms $-\partial uz/\partial x$ and $-\partial vz/\partial y$ almost balance at the 100th day, but the two nonlinear terms show poor compensation afterward. The initial current path along the boundary is unstable in Run 11 and it gives rise to another current path pattern. In comparison with the vorticity balance found in Runs 8 and 9, the results of Run 11 suggest that small horizontal dissipation gives favorable condition for the occurrence of instability of the initial coastal flow along the northern boundary. From the above numerical experiments, it results that the appearance of a meander path along the larger coastline inclination is possible, if both a small horizontal dissipation and large in- and out-flow are employed. It is also pointed out that the formation of the meander path is necessarily associated with the instability of the western boundary current along the coastal boundary.

4. Summary and discussion

The Kuroshio region south of Japan has some characteristic topographies in comparison with the

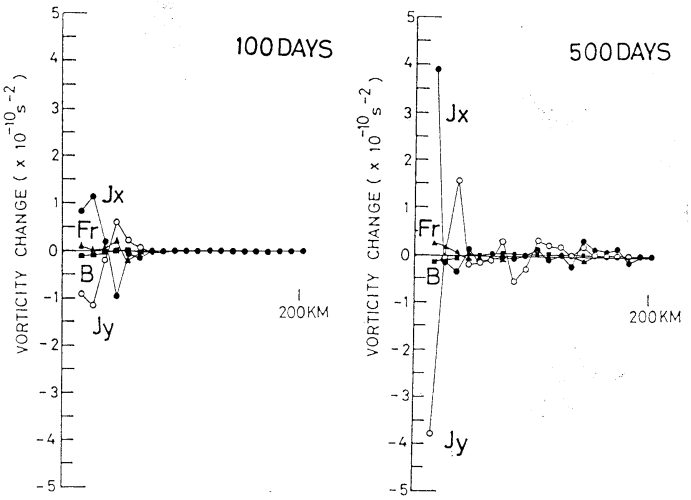

Fig. 11. The same as in Fig. 9, but for 100th day and 500th day of Run 11.

other western boundary region; a relatively small coastline inclination, narrow continental slope and the Izu Ridge. On the basis of the observational evidence that the large meander path is peculiar to the Kuroshio, the effects of coastline inclination from W-E direction and the continental slope on the western boundary current have been studied in the present study. The main results are summarized as follows:

(1) A western boundary current along a smaller coastline inclination from W-E direction is unstable and it has a tendency to take a meander path. This is due to larger eastward advection of the relative vorticity by the mean flow, which becomes large as the coastline inclination becomes small.

(2) The formation of the large meander path is suppressed by the topographic effect of the continental slope. If the topographic effect of the continental slope is predominant, no large meander path is formed along a zonal northern boundary and a current apts to flow along an isopleth of the depth. The narrow continental slope south of Japan and resulted small topographic effect of the slope in comparison with the other western boundary are supposed to be associated with the appearance of the large meander path.

(3) From the results of Runs 1 and 2, it has been pointed out that if the coastline inclination is included, the stationary Rossby wave theory (e.g., WHITE and MCCREARY, 1976) is not suitable and the wavelength of the stationary Rossby wave is greatly influenced by the effect of northern boundary. A western boundary current is strongly deformed at the western north corner of the basin and the vorticity exchange with the boundary is important in this process.

(4) In the case with a large coastline inclination from W-E direction, large meander path is not formed even if a very large in- and outflow volume transport is given (Runs 8 and 9). However, if the small coefficient of eddy viscosity is imposed (Run 11), a current path separation from the northern boundary is carried out. It is inferred from these models that the instability of the coastal current path is more sensitive to the eddy viscosity than to the nonlinear effect.

It has been suggested by Fig. 3 that there exists a critical coastline inclination from W-E direction between those of Run 2 and Run 3 that divides approach or separation of a western boundary current from a coastal boundary. Because the coastline inclinations of Runs 2 and 3 represent the actual tilts of the coasts from Shikoku to Boso Peninsula and the total from south of Kyushu to Boso Peninsula, respectively, the results of Fig. 3 agree with the observational evidence that the large meander of the Kuroshio is observed in the former area, where the incli-

nation of the coast is relatively small. Although generation of a small meander is frequently observed off Kyushu, they are caused by the abrupt increase in the current velocity of the Kuroshio (SEKINE and TOBA, 1981a, b). If a stationary current velocity is assumed, the Kuroshio path off Kyushu has a tendency to flow along a coastal boundary (SEKINE and TOBA, 1980).

Next, we refer to the future problems of the coastal and bottom topographic effects on the path dynamics of the Kuroshio. In the present study, the latitude of the outflow has been fixed, but there is a possibility that the path character along a constant coastline inclination is changed if the outflow latitude is changed. The numerical experiments by YOON and YASUDA (1987) showed that in a model with 23 degrees coastal inclination ($A_h=8\times10^5$ $cm^2\ s^{-1}$), a large meander path is formed if the volume transport is greater than 40 Sv. However, the present model showed that meander path is not formed in the Runs 3, 4, 8 and 9. This discrepancy is due to the difference in latitudinal distance of the inflow and outflow; the latitudinal distance of the present model is 710 km, whereas that of YOON and YASUDA (1987) model is 350 km. If the latitudinal distance is small, the effect of coastline inclination on the current path is decreased. Therefore, the latitude of the outflow is supposed to be an important factor of the path dynamics and this problem will be examined in succeeding paper (SEKINE, MS). Furthermore, the present study has shown that even if the outflow latitude is fixed, the path character is changed by the intensity of topographic effect of the continental slope and eddy viscosity. As for these problems, observational parameterization has not been well carried out. It is strongly needed to do observational parameterization for drawing a firm conclusion on the path dynamics of the Kuroshio south of Japan.

Acknowledgments

I would like to thank Professors Y. TOBA of Tohoku University, K. TAKANO of Tsukuba University and N. SUGINOHARA of University of Tokyo, and Drs. J.H. YOON and M. FUKASAWA of University of Tokyo for their helpful discussion and comments. The numerical calculations were carried out on a HITAC M-200H in the Computer Center of National Defense Academy.

References

BRYAN, K. (1963): A numerical investigation of a nonlinear model of a wind-driven ocean. J. Atmos. Sci., **20**, 594-606.

CHAO, S-Y. and J.P. MCCREARY (1982): A numerical study of the Kuroshio south of Japan. J. Phys. Oceanogr., **12**, 680-693.

CHAO, S-Y. (1984): Bimodality of the Kuroshio. J. Phys. Oceanogr., **14**, 92-103.

ENDOH, M. (1973): Western boundary current crossing a ridge—barotropic model and equivalent barotropic models—. J. Oceanogr. Soc. Japan, **29**, 140-147.

ENDOH, M. (1978): Effects of a marine ridge to western boundary current in a three-dimensional source-sink flow model. J. Oceanogr. Soc. Japan, **34**, 303-306.

FUKASAWA, M. and T. TERAMOTO (1986): Characteristics of deep currents off Cape Shiono-misaki before and after formation of the large meander of the Kuroshio in 1981. J. Oceanogr. Soc. Japan, **42**, 53-68.

ISHII, H., Y. SEKINE and Y. TOBA (1983): Hydrographic structure of the Kuroshio large meander-cold water mass region down to the deeper layers of the ocean. J. Oceanogr. Soc. Japan, **39**, 240-250.

KAWABE, M. (1985): Sea level variations at the Izu Islands and the typical stable paths of the Kuroshio. J. Oceanogr. Soc. Japan, **41**, 306-326.

MASUDA, A. (1982): An interpretation of the bimodal character of the stable Kuroshio path. Deep-Sea Res., **29**, 471-484.

MATSUNO, T. (1966): Numerical integration of the primitive equations by a simulated backward difference method. J. Meteor. Soc. Japan, **44**, 76-84.

MIURA, H. and N. SUGINOHARA (1980): Effects of bottom topography and density stratification on the formation of western boundary currents. J. Oceanogr. Soc. Japan, **35**, 215-223.

MUNK, W.H. (1950): On the wind-driven ocean circulation. J. Meteorol., **7**, 79-93.

MUNK, W.H., G.W. GROVES and G.F. CARRIER (1950): Note on the dynamics of the Gulf Stream. J. Mar. Res., **9**, 218-238.

NISHIDA, H. (1982): Description of the Kuroshio meander in 1975-1980: Large meander of the Kuroshio in 1975-1980 (I). Rep. Hydrogr. Res., (17), 181-207.

OTSUKA, K. (1985): Characteristics of the Kuro-

shio in the vicinity of the Izu Ridge. J. Oceanogr. Soc. Japan, **41**, 441-451.

ROBINSON, A.R. and B. TAFT (1972): A numerical experiment for the path of the Kuroshio. J. Mar. Res., **30**, 65-101.

SEKINE, Y. (1979): A numerical experiment for bottom effect of the Izu Ridge on path of the Kuroshio I. Barotropic stationary model. Sci. Rep. Tohoku Univ., Ser. 5, Geophys., **26**, 67-80.

SEKINE, Y. (1980): A numerical experiment for bottom effect of the Izu Ridge on path dynamics of the Kuroshio II. On the formation of stationary path with an increase in volume transport. Sci. Rep. Tohoku Univ., Ser. 5, Geophys., **27**, 19-25.

SEKINE, Y. and Y. TOBA (1980): A numerical study on path of the Kuroshio with reference to generation of small meanders southeast of Kyushu. Sci. Rep. Tohoku Univ., Ser. 5, Geophys., **27**, 39-55.

SEKINE, Y. and Y. TOBA (1981a): Velocity variation of the Kuroshio during the formation of the small meander south of Kyushu. J. Oceanogr. Soc. Japan, **37**, 87-93.

SEKINE, Y. and Y. TOBA (1981b): A numerical study on the generation of the small meander of the Kuroshio off southern Kyushu. J. Oceanogr. Soc. Japan, **37**, 234-242.

SEKINE, Y. (1984): Coastal and bottom topographic effect on the path of the Kuroshio. Mar. Sci., **17**, 283-292 (in Japanese).

SEKINE, Y. (1989a): Formation process of the large meander of the Kuroshio south of Japan. (submitted to Deep-Sea Res.)

SEKINE, Y. (1989b): A numerical experiment on the path dynamics of the Kuroshio with reference to the formation of the large meander path south of Japan. (submitted to Deep-Sea Res.)

STOMMEL, H. and K. YOSHIDA (1972): Kuroshio -Its physical aspects. Univ. of Tokyo Press, Tokyo. 517 pp.

TAFT, B.A. (1972): Characteristics of the flow of the Kuroshio south of Japan. p. 165-214. *In*: H. STOMMEL and K. YOSHIDA (ed.), Kuroshio -Its physical aspects. Univ. of Tokyo Press, Tokyo.

VERONIS, G. (1966): Wind-driven ocean circulation: Part II. Numerical solutions of the non-linear problem. Deep-Sea Res., **13**, 31-55.

WHITE, W.B. and J.P. MCCREARY (1976): The Kuroshio meander and its relationship to the large-scale ocean circulation. Deep-Sea Res., **23**, 33-47.

YASUDA, I., J.H. YOON and N. SUGINOHARA (1985): Dynamics of the Kuroshio large meander -barotropic model-. J. Oceanogr. Soc. Japan, **41**, 259-273.

YOON, J.H. and I. YASUDA (1987): Dynamics o the Kuroshio large meander. Two-layer model. J. Phys. Oceanogr., **17**, 66-81.

日本南岸の黒潮に注目した西岸境界流の流路に及ぼす陸岸・海底地形効果

関　根　義　彦

要旨：日本南岸の黒潮流域は他の西岸境界流流域と比較して，東西方向からの陸岸線の傾きが小さく，陸棚斜面の幅が狭いという特徴がある。黒潮流路は大蛇行流路と非大蛇行流路との間に二様性を示すが，ほかの西岸境界流には大蛇行流路が観測されない。そこで，陸岸・海底地形が黒潮流路に及ぼす影響を順圧数値モデルを用いて調べた。平坦なモデルでは陸岸が東西方向に近くなるにつれて，西岸境界流が蛇行しやすく，反対に南北に走る岸では西岸境界流が接岸する傾向が強いことが示された。とくに後者では，大きな流量と小さな粘性係数が与えられれば接岸流路の不安定が生じ，流れは離岸する。大陸棚の海底地形を考慮したモデルでは，流れが等地衡値（f/h, f はコリオリのパラメータ，h は水深）に沿う性質により，大蛇行の形成は押さえられる。これらより，大蛇行流路の形成は岸に沿う粘性境界流が不安定になることに関連することが示唆される。もし不安定が生じ，一般流によって東に移流された相対渦度が西向きのロスビー波とバランスすれば，大蛇行流路が形成される。これらの結果は東西方向に近い陸岸地形と狭い大陸棚斜面を持つ日本南岸では蛇行が発生しやすいことを示す。